Indian Journal of Fundamental and Applied Life Sciences ISSN: 2231– 6345 (Online)
An Open Access, Online International Journal Available at www.cibtech.org/sp.ed/jls/2015/03/jls.htm
2015 Vol. 5 (S3), pp. 102-111/Joodaki and Karimi

Research Article

MINERALOGY, LITHOLOGY AND GEOCHEMISTRY OF SIAHKOOH IRON ORE DEPOSIT (YAZD, IRAN)

Mina Joodaki and *Mehrdad Karimi
Department of Geology, College of Sciences, Shiraz Branch, Islamic Azad University, Shiraz, Iran
**Author for Correspondence*

ABSTRACT

This case study is a part of Siahkooh national park in Yazd province. Rock formation consists of sprite limestone, dolomitic limestone and young Quaternary alluvium, and igneous masses of granite, diorite, monzodiorite to olivine gabbro have intruded into older limestones in this area. This ore body is an epigenetic deposit and infilling voids and substitution is visible in it. This deposit contains hematite, goethite, oligiste, pyrite, chalcopyrite, malachite, bornite, chalcocite and covellite, which are in the form of veinlets, veins and stockworks. Substitution and infilling voids are the most important features of hematite and oligiste. Overall, significant anomalies of iron, copper, lead, zinc, silver, barite, arsenic and uranium are seen in the Siahkooh index. Alteration and fragmentation pattern of metals in ore samples of Siahkooh deposit are very similar to hydrothermal iron deposits in the world; moreover, the amount of magma elements including titanium, chromium, vanadium, cobalt, nickel and phosphorus in the ore body is very low, which is a proof for the function of ore-bearing fluid in the Siahkooh area.

Keywords: *Yazd, Siahkooh, Iron Ore, Hydrothermal System, Geochemistry*

INTRODUCTION

The study area is located in 32° 35' N and 53° 59' E, and is a part of Siahkooh national park in Yazd province, central Iran.

The access road to the area is via Ardakan-Choopanan paved road. The study area is a part of central Iran structural zone and sedimentary sequences from the upper Precambrian to the present age are exposed in this zone.

From morphological point of view, Siahkooh national park has all three units of mountains, plains and playa.

Geologically, rock formation of the area consists of sandstone, siltstone, dolomitic limestone and sprite limestone in Jurassic and Cretaceous age and Quaternary alluvium (Figure 1).

In this area, igneous masses of granite, diorite, and monzodiorite to gabbro have intruded into older rocks. Many studies have been done on Siahkooh desert, including Dehghani (1991) who carried out a geological survey on sediments and their importance and geomorphology in Siahkooh desert.

He has also interpreted and analyzed minerals in Ardakan Playa with an emphasis on economic importance of each of them in 2000 after considering the types of sub-environments in Playa and geomorphic effects of them.

Regional Water Company in 1998 presented a statistical report on the balance of the groundwater of Siahkooh desert sub- basin.

Although extensive studies have been done on iron deposits in Yazd province, no formal academic research has been done on the geology, mineralization and genesis of deposits in the Siahkooh area, therefore the present studies are new and very valuable. The aim of the present paper is to study mineralogy, lithology and geochemical conditions prevailing in the formation of iron and barite ore in the Siahkooh area.

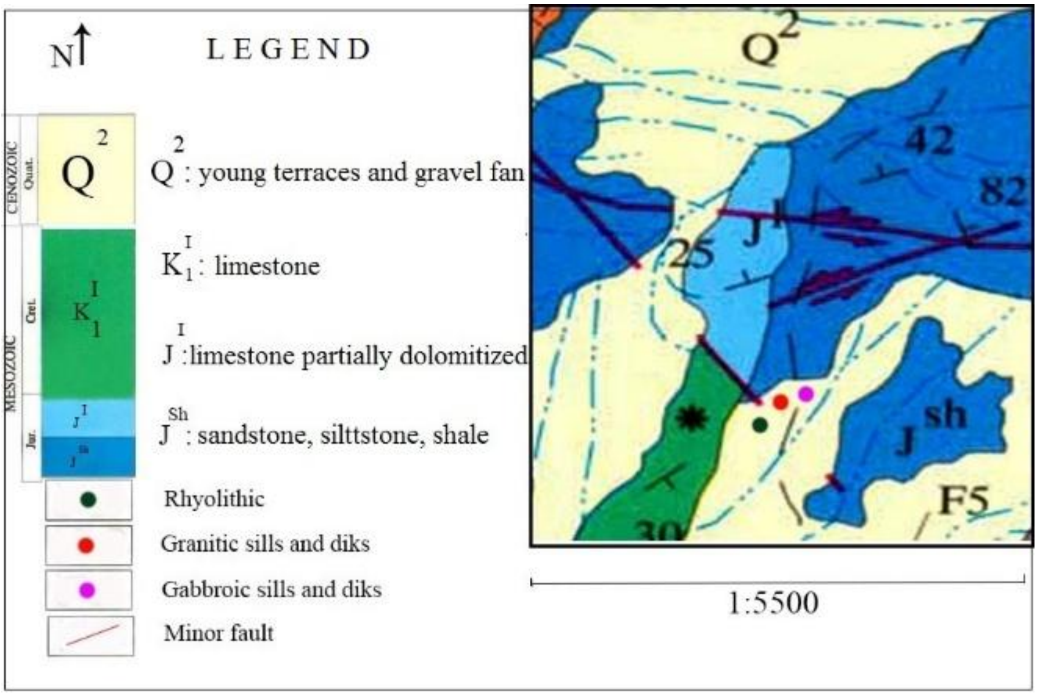

Figure 1: Geology map of the study area

RESULTS AND DISCUSSION

Discussion

Lithology. Based on field studies, rock formation of the area includes sprite limestone, dolomitic limestone, young Quaternary alluvium, alkali granite, olivine gabbro, granite porphyry and diorite. 16 thin sections were prepared from the ore sample and its host rock. The host rock is mainly sprite limestone and dolomitic limestone in some parts with Jurassic and Cretaceous age. According to microscopic studies various minerals of calcite, dolomite, quartz, amphibole, plagioclase, biotite, chlorite, olivine and epidote have been seen in limestones and igneous masses. Some relatively tiny grains of opaque minerals which are possibly pyrite, in the form of hexagonal are scattered in many parts of sprite limestone. Evidences indicate the influence of a Fe-bearing fluid into the host rock fractures that has deposited iron oxide minerals in it. The impact of this fluid in sprite and dolomitic limestone is much more than other areas. Fractures of microsprite limestone are filled with secondary quartz and calcite as sprite. It is thought that the secondary calcite and quartz have entered into these fractures through hydrothermal fluids. Igneous rocks in the study area consist of felsic-intermediate to mafic rocks including diorite, leucogranite, and monzodiorite olivine gabbro. What is remarkable in these rocks is their extreme alteration, so that in some rocks plagioclase has been altered and almost gone and zoning is not seen. Secondary minerals of intermediate rocks are often chlorite and epidote. In granites of the study area orthoclase crystals have been greatly disintegrated into clay minerals such as kaolinite and sericite. Tiny crystals of epidote family can be seen in some thin sections. A brief description of each rock formation is presented below:

Olivine gabbro is made of olivine, plagioclase and clinopyroxene. Most clinopyroxenes are augite and plagioclases are often labradorite and bytownite. Olivine minerals are often regular and shaped, and some of them have located in plagioclase minerals. Opac minerals have been made in pyroxene and olivine texture (Figure 2 A).

Diorite is often altered and the main rock-forming minerals are plagioclase and amphibole and secondary minerals are generally epidote and very small amount of chlorite. Plagioclase in this rock has been altered and almost gone and zoning has not been seen, and about 2 to 3 % of this rock is formed by opac stretched minerals and these stretched minerals located in the plagioclase are most likely iron oxide (Figure 2 B).

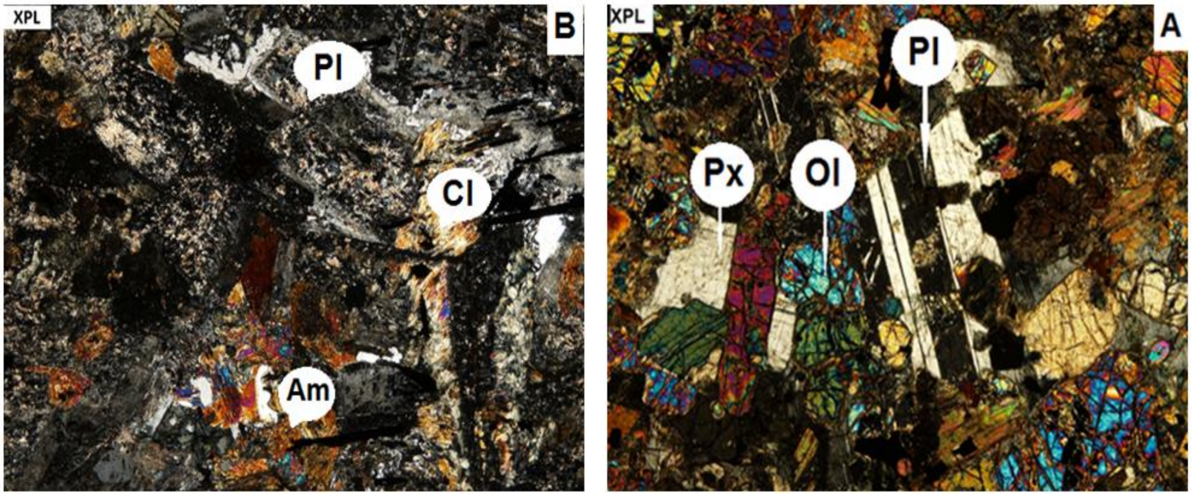

Figure 2: A) Olivine, pyroxene and plagioclase in olivine gabbro with a magnification of 40; B) Amphibole, plagioclase and chlorite in diorite with a magnification of 40

In microdiorite, crystals are relatively fine and the grain size is about one millimeter. The grain size in this rock shows that they are made in a semi-deep area such as diabase bodies; however, the point of difference lies in the fact that diabases are rich in pyroxene, while the studied sample contains plagioclase and amphibole, so the studied rock is considered as a microdiorite. Secondary minerals are calcite, chlorite and epidote. The rock is fairly severely altered as so most amphiboles have been chloritic.
Leucogranite is mostly composed of orthoclase crystals. Orthoclase crystals are mainly altered into clay minerals such as kaolinite and sericite. Quartz minerals are in myrmekitic and graphics texture in this rock. Opac minerals in this rock are made of biotite which are often shaped and partly altered to chlorite (Figure 3).

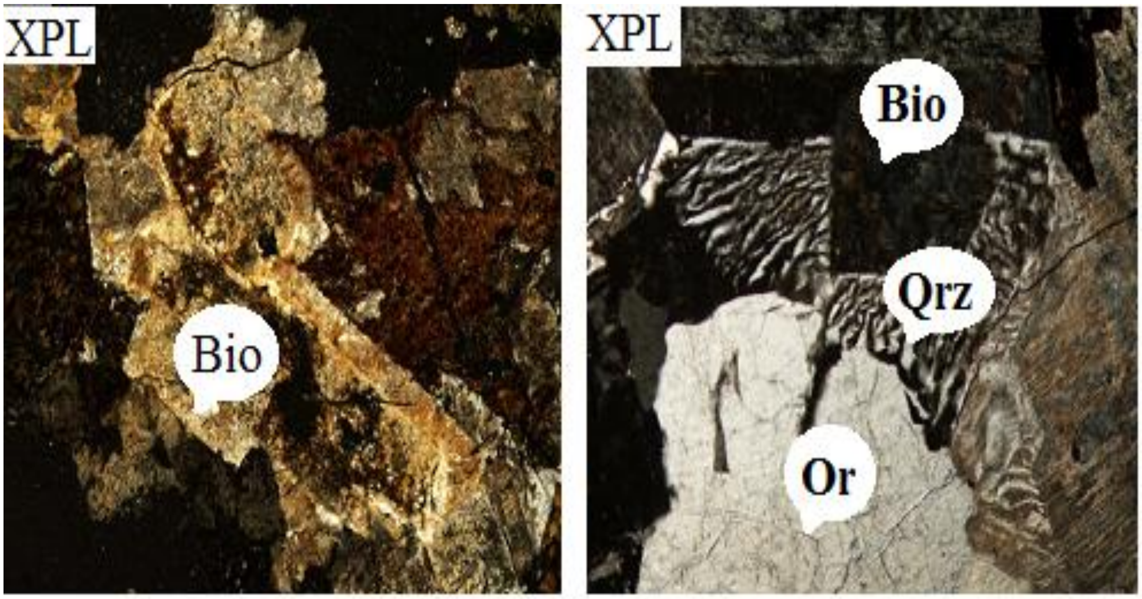

Figure 3: Quartz, biotite and orthoclase in leucogranite with a magnification of 40

Microsprite limestone whose fractures are filled with secondary quartz and calcite as sprite. It is thought that secondary calcite and quartz have been entered into these fractures through hydrothermal fluids (Figure 4).

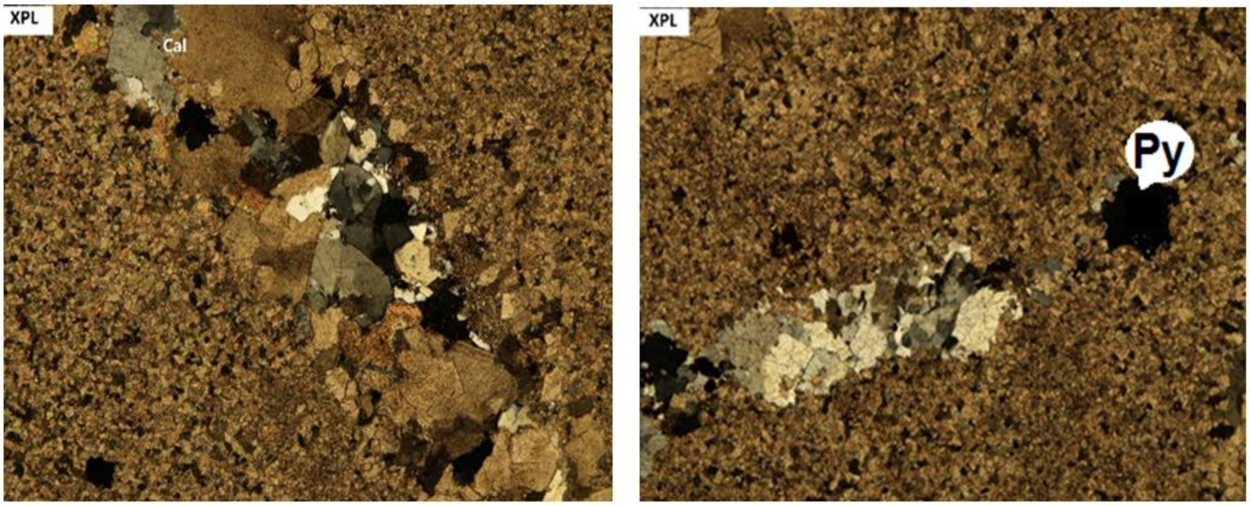

Figure 4: Fracture-filling of sprite limestone by secondary quartz, calcite and a few pyrites with a magnification of 40

Mineralogy

Microscopic studies and XRD data (Table 1) indicate that Siahkooh iron ore has a variety of mineralogy and extended mineralization; the spread of alteration, confirms this issue. Oxidation to hematite, goethite and limonite is frequently observed along fractures and cracks especially in the surface which caused a gossan zone with high percentage of iron oxide. This issue probably indicates that there is an enormous amount of sulfide minerals in the area which is a confirmation of the extended mineralization. Under the microscope, hematite seems as a large dimension blade with the size of 0.5 to 1 cm. also, the hematite particles in some sections created a spongy and rhythmic texture (Figure 5A) which indicates it has been formed in low temperature. In samples where the hematite is replaced by pyrite (Figure 5 B), internal structure and crystal shape are retained. Bubble texture observed in sections shows decomposition of a mineral and substitution of iron oxide. Hydrous iron oxides (goethite and limonite), among the secondary minerals, are the most abundant which are frequently observed in sections (Figure 5E). A large part of host rock is impregnated with iron because of the influence of iron-rich fluid at the surface (Figure 5F). Goethite is the most stable iron hydroxide (Torabian, 2007) which is observed as rhythmic and granular texture in the section due to dissolution and oxidation phenomenon. Sulfide minerals (pyrite and chalcopyrite) are widely seen together with iron oxide as scattered and in the form of veins and veinlets that shows final stages of hydrothermal fluid activity (Marschik *et al.*, 2008) and usually are altered to iron oxides and iron hydroxides in surface oxidation conditions.

Table 1: The results of XRD analysis

Sample	Major phase	Minor phase	Trace phase
Sk-178-2	Kaolinite	Natroalunaite- Illite- Goethite- Anatase- Quartz- Halite	.....
Sk-129-2	Hematite- Quartz	.....	.....
Sk-178-1	Hematite- Quartz	.....	.....
Sk-178-3	Quartz- Goethite	Halite	Hematite
Sk-175-1	Malachite	Quartz- Goethite	....
Sk-174-1	Dolomite- Barite- Quartz	Calcite	....
Sk-129-3	Hematite- Quartz	Rutile- Kaolinite- Magnetite	....
Sk-174-3	Barite- Quartz	Calcite- Ankerite	....
Sk-178-4	Quartz- Muscovite - illite - Goethite	Albite- Tormaline	Halite
Sk-180-1	Quartz- Illite- Calcite	Kaolinite- Albite	....

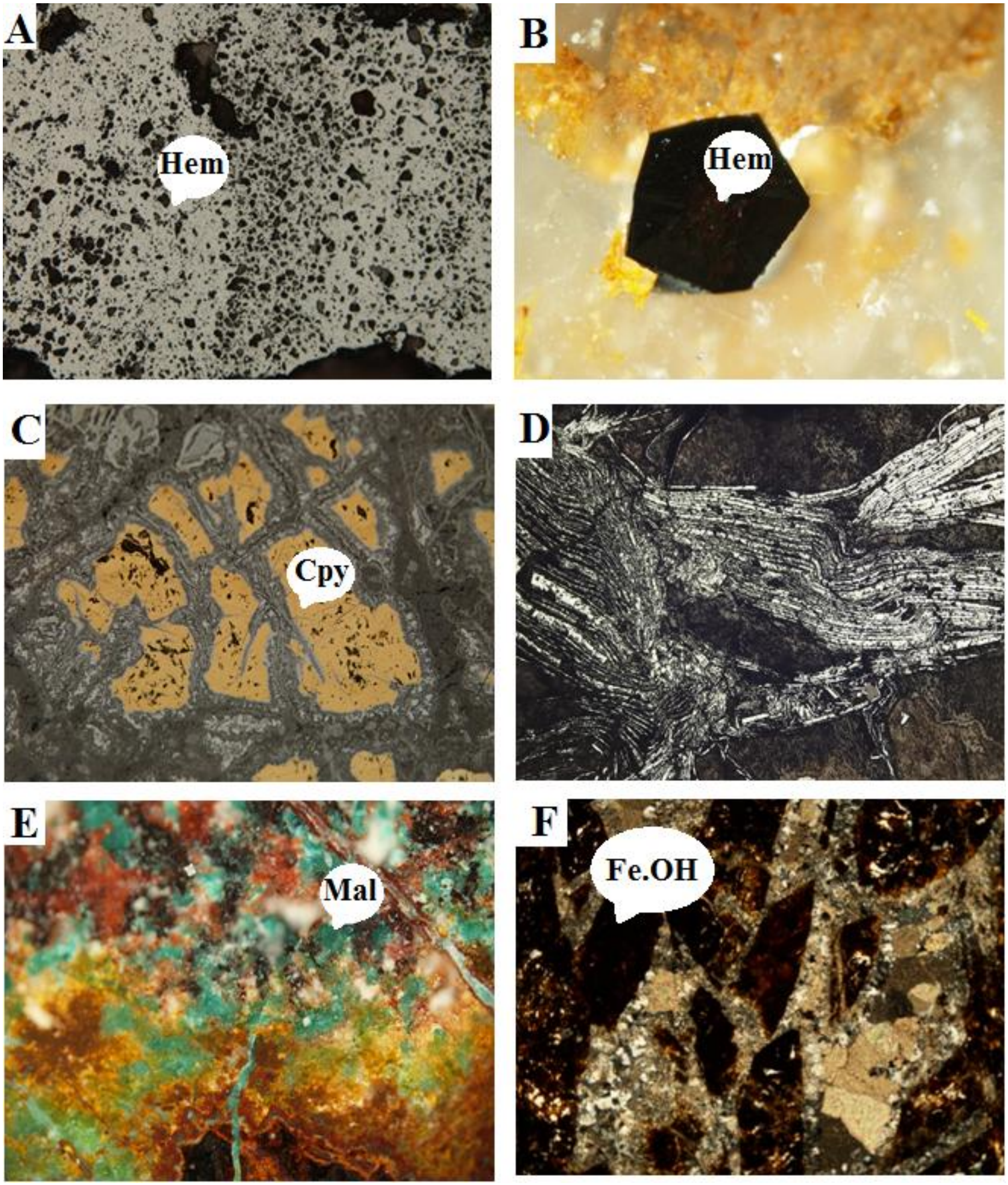

Figure 5: A) Fine and relatively coarse crystals of hematite and creating spongy texture with a magnification of 100. B) Regular geometric shape of pyrite crystal is filled by hematite, with a magnification of 200. C) Fracturing and corrosion of chalcopyrite crystal and formation of island texture, with a magnification of 100. D) Oligiste blades are folded and fully stretched in goethite, with a magnification of 100. E) Goethite with malachite, with a magnification of 100. F) Reaction of hydrothermal solution silica and iron oxide-rich with a mass of carbonate, with a magnification of 40

Pseudosuccessor texture of pyrite in addition to chalcopyrite corrosion by hematite confirms this issue (Figure 5C). Also, the presence of traces of silica and calcite in the form of veins and veinlets crossover deposits and the host rock represents the final stages of hydrothermal fluid activity. Oligiste blades are relatively frequently observed in polished sections. Some blades are twisted which indicates tectonic stress on the ore body (Figure 5D). Some blades are as broom handle and some others are box texture and the spaces between boxes are filled with goethite. Malachite, chalcocite, covellite, bornite and chrysocolla are the secondary minerals observed in polished sections that indicate contamination of iron ores by copper.

Geochemistry

A number of thirty samples including host rock, ore and rocks altered by hydrothermal fluids were taken for geochemical study on Siahkooh index. Sampling was done sporadically due to conditions prevailing in the area including lack of access roads and also being protected by Environmental Protection Agency of Yazd province. Finally, selected samples of the study area were analyzed using XRF and ICP methods in Kansaran-E Binalood laboratory and the results of the analysis of the main elements are shown in Table 2 and 3.

Table 2: The results of XRF

Sample%	SK-180-1	SK-179-1	SK-187-1	SK-178-1	SK-129-6	SK-175-2	SK-175-3	SK-176-1	SK-129-2	SK-129-3	SK-129-4	SK-129-5	SK-173-8	SK-173-9
SiO_2	54/36	26/42	0/26	20/67	7/39	1/68	0/53	0/54	6/95	42/81	43/62	27/19	1/24	47/62
Al_2O_3	14/39	2/74	0/09	0/26	0/52	0/16	0/1	0/11	1/67	2/17	1/96	1/73	0/14	8/1
Fe_2O_3	4/01	68/91	76/89	75/81	90/21	96/84	73/29	2/76	86/34	47/34	52/39	48/19	0/06	26/58
CaO	9/03	0/07	0/83	0/03	0/13	0/04	11/45	0/45	0/12	0/06	0/03	0/02	0/86	1/74
Na_2O	0/39	0/04	0/06	0/02	0/02	0/02	0/04	0/03	0/04	0/04	0/1	0/03	0/03	0/11
K_2O	3/42	0/82	0/03	0/01	0/05	0/02	0/04	0/03	0/47	0/21	0/15	0/29	0/02	2/38
MgO	1/25	0/16	0/62	0/02	0/02	0/02	2/27	0/03	0/13	0/07	0/03	0/05	0/03	0/48
TiO_2	0/573	0/14	0/005	0/024	0/143	0/003	0/002	0/087	0/031	2/804	0/15	0/041	0/082	1/137
MnO	0/053	0/003	0/893	0/004	0/019	0/012	0/49	0/005	0/023	0/006	0/02	0/004	0/003	0/015
P_2O_5	0/084	0/003	0/012	0/024	0/048	0/009	0/005	0/005	0/005	0/096	0/027	0/007	0/003	0/153
S	0/005	0/003	8/96	0/171	0/055	0/029	0/005	32/89	0/834	0/975	0/188	6/956	33/02	1/754

Table 3: The results of ICP

Sample%	SK-187-1	SK-175-1	SK-175-2	SK-174-1	SK-173-1
Ag	4/4	21.5	0/5	2/8	0/23
Ba	1796	115	914	2399	393
Cu	53431	142966	23	98	28
Fe	>10%	>10%	>10%	42619	14870
Pb	222	80	85	6	4
Zn	1276	755	66	19	17
As	763	40/6	1/9	2/4	8/1
P	183	955	174	120	229
S	>3%	10893	364	3694	545
U	10/2	9/2	8/1	3/9	22

Iron: Amount of this element varies from 2 to 97%. The maximum amount of it can be seen in the east part of the mine and in the limits of the alterations. This element is mostly in the form of hematite, goethite, limonite and oligiste (Figure 7a).

Copper: The amount of this element varies from 9 to 142966 ppm. This element is mostly in the form of malachite and chalcopyrite and a lesser amount of chalcocite, covellite and bornite (Figure 6d). Carbonate compounds are formed in low temperature deposit at surface and under oxidation conditions (Guilbert and Park, 1997).

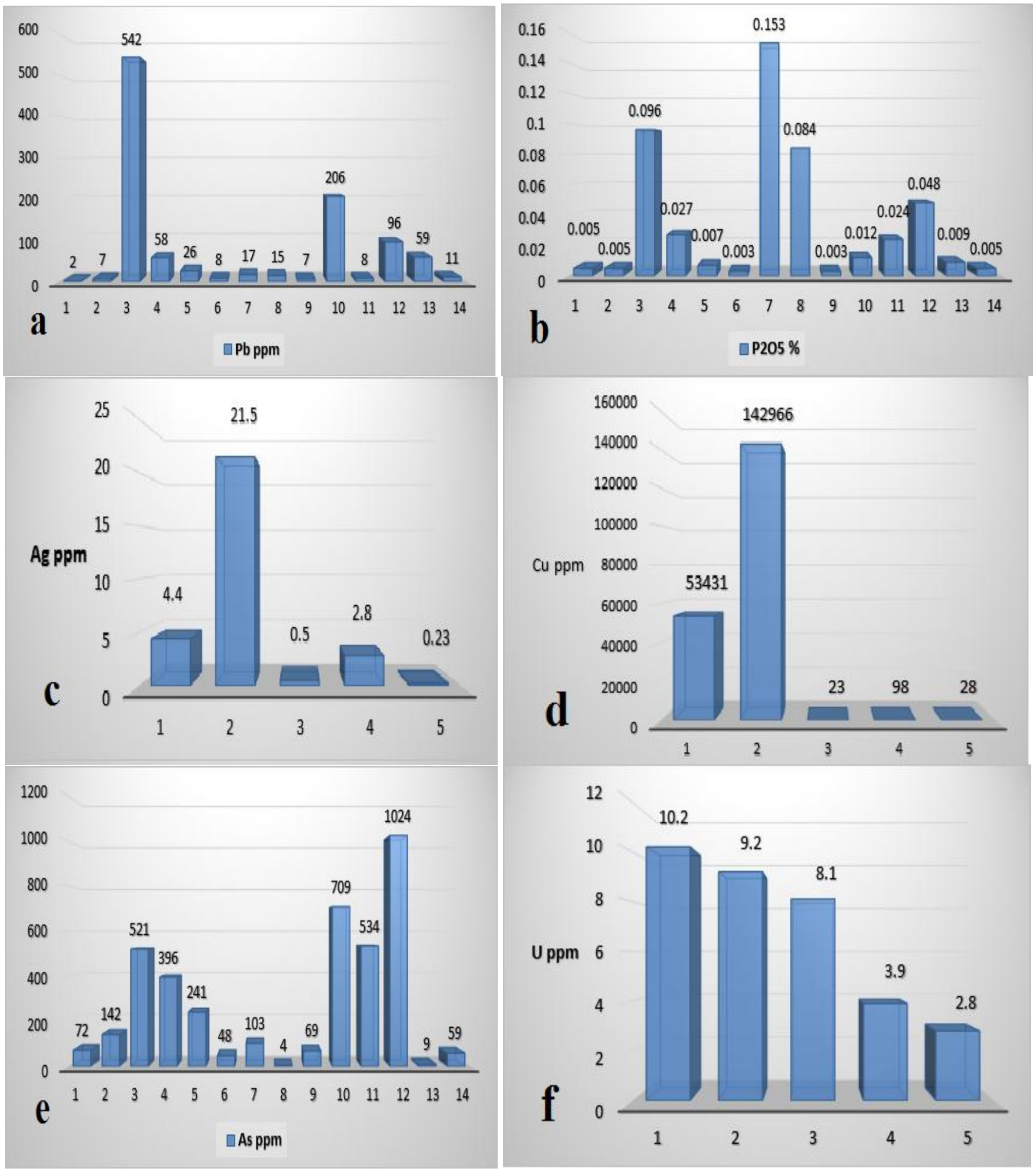

Figure 6: Frequency diagram of lead, uranium, arsenic, silver, phosphorus and copper

Silver: The amount of this element varies from 0.5 to 2.5 ppm. The maximum amount of it is seen in copper-rich ore. This element is widely carried by chloride complexes (Robb, 2005), silver is a by-product associated with iron mineralization in hydrothermal deposits (Williams *et al.*, 2005) and sediments in alkaline and reduction conditions (Figure 6c).
Arsenic: It varies from 1.9 to 1024 ppm. The minimum of it is seen in oligiste-rich ore and the maximum is seen in ore containing hematite and goethite (Figure 6e).
Lead: It varies from 2 to 542 ppm. The maximum amount of it can be seen in gossan zone (Figure 6a).
Zinc: This element varies from 12 to 276 ppm. The maximum of it presents in chalcopyrite and iron-rich ore.

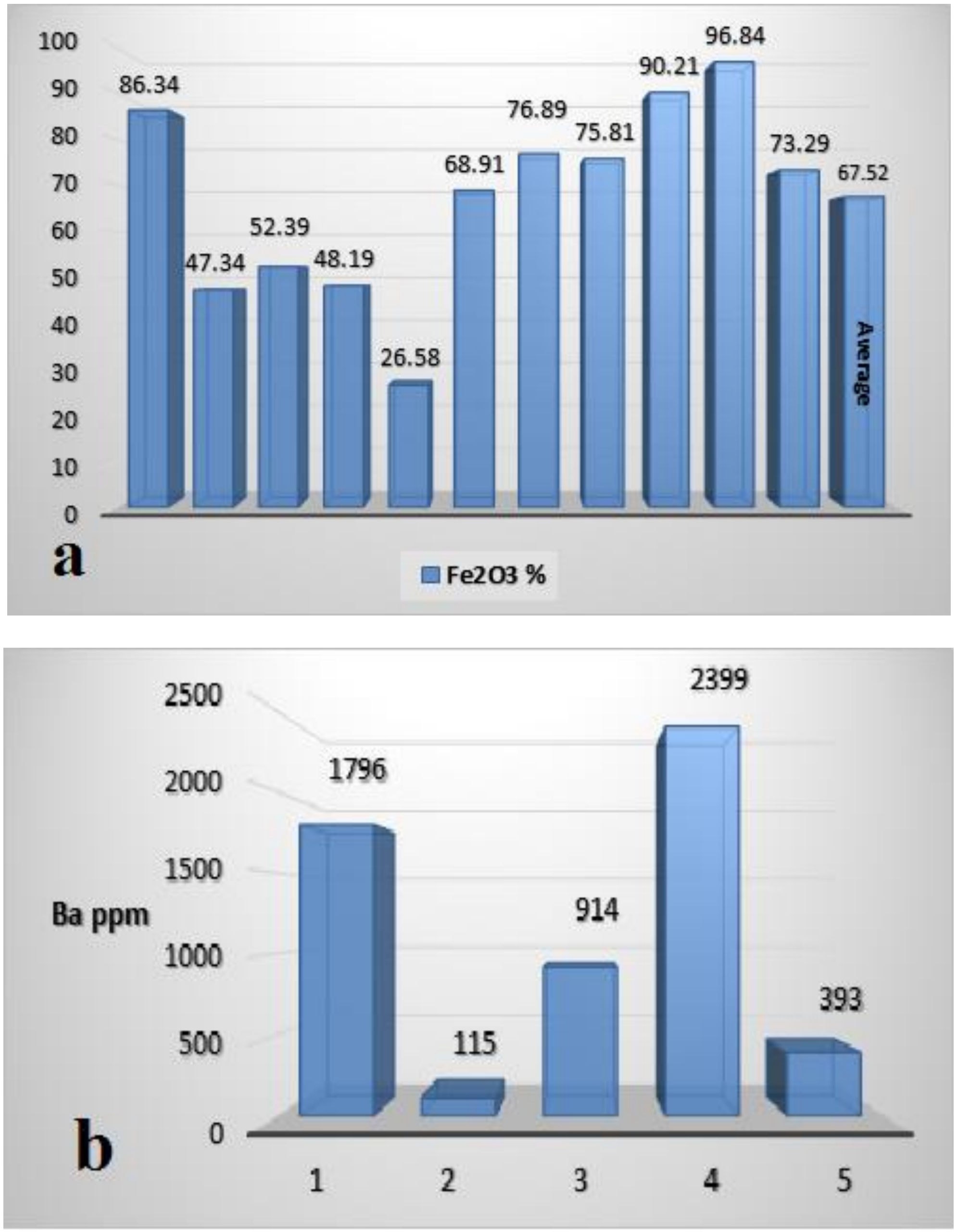

Figure 7: a) Frequency diagram of iron oxides in iron ore, b) Barium frequency diagram

Barium: It varies from 32 to 628400 ppm. The maximum amount is seen in barite veins and veinlets (Figure 7b). Barite in deposit is as the final phase of mineralization with vein construction and fracture filling texture and is the product of a hydrothermal fluid deposition in an average temperature (Gholami, and Aftabi, 2010).

Uranium: It varies from 1 to 10.2 ppm. The maximum amount is seen in iron and chalcopyrite rich ore (Figure 6f).

Phosphorous: The level of phosphorous is low in most samples. It can be concluded that if the ore was formed by magmatic segregation, then the P content in the samples would be very high (Figure 6b).

In general, significant anomalies of iron, copper, lead, zinc, silver, arsenic and uranium are seen in Siahkooh index. Since iron has formed an ore in hydrothermal range as iron oxide (gossan), thus it shows a negative or very weak correlation with lead, zinc and copper which are formed as carbonates and sulfides (Figure 8 a., b., c). Moreover, the positive correlation between sulfur and barium shows that barium has economic importance in composition with sulfur (barite) (Figure 8d). Weak correlation between sulfur and iron can also indicate the non-magmatic origin of iron. The ratio of Fe/Mn highly varies in hydrothermal deposits and includes quantities more than 10 to values smaller than 0.1. This issue implies erratic differentiation of iron and manganese in the sedimentary environment of these deposits (Bonatti *et al.*, 1972). In sedimentary environment manganese can be isolated due to further geochemical mobility; this means that iron is less soluble than manganese and deposits faster (Roy, 1980). Since Al and K were not active in hydrothermal processes and are usually provided from epeirogeny origin, so, it can be concluded that these elements are epeirogenic (Crerar *et al.*, 1982).

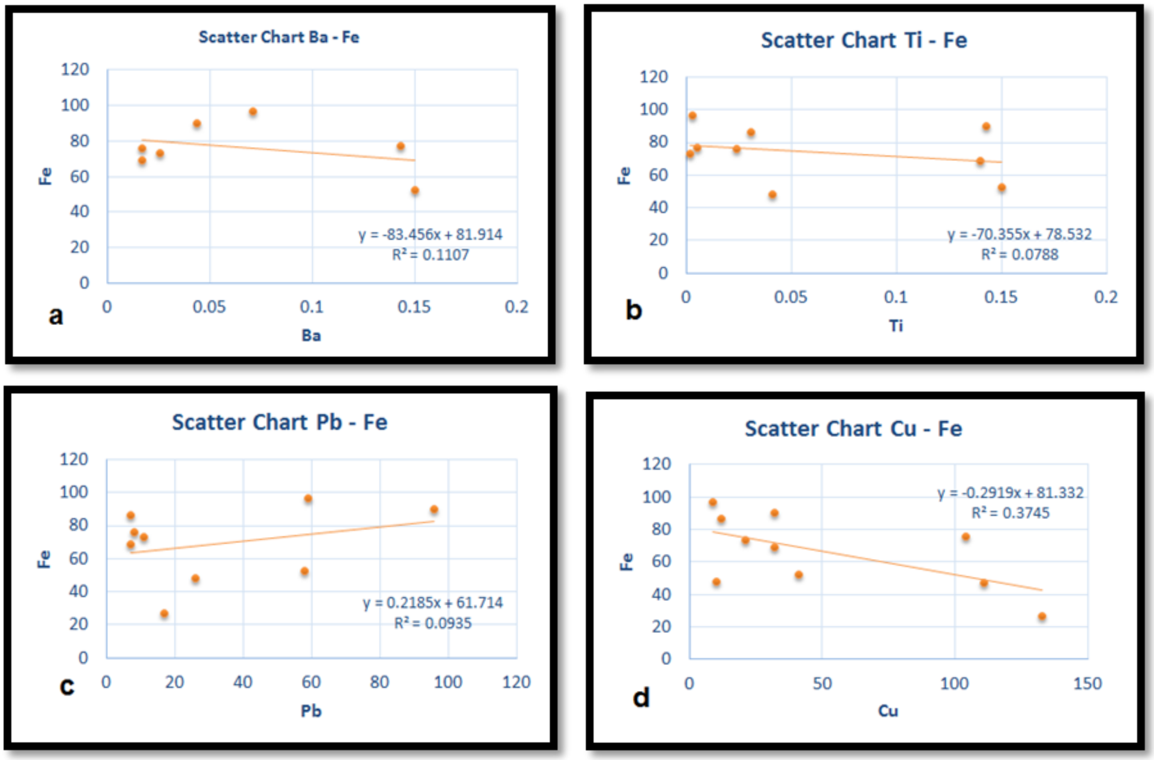

Figure 8: Correlation diagram of barium, titanium, lead, copper with iron

Conclusion

Rock formation of the study area consists of sprite limestone, dolomitic limestone, and young Quaternary alluvium, igneous masses of granite, diorite, and monzodiorite to olivine gabbro. Siahkooh iron index is typically associated with igneous activity. Deposition in this index is epigenetic and infilling voids and substitution is visible in them. Mineralization is seen in the form of veins and stock works and the main minerals are sulfides of copper, lead, zinc and silver, iron oxide and carbonate of copper. Abundant oxide and hydroxide minerals in the upper levels of deposit with the texture of bubble, box, and pseudomorph indicate wide activity of hydrothermal fluid and pyrite and chalcopyrite oxidation. Substitution and infilling voids is one of characteristics of hydrothermal iron ore. It should be noted that some hematite minerals can be crystalized in low temperature in final stages of hydrothermal fluid during rapid cooling and instability of iron-bearing complexes. In mineralogical data no crystal composition which is an indicator of skarn environment has been found. According to the statistical analysis of the results the amount of iron oxide (Fe_2O_3) is significant and varies from 26 to 97%; therefore iron is the most important economical element in upper level of the ore which is presented as hematite, goethite, limonite and oligiste. Substitution and infilling voids is the most important feature of hematite and oligiste. Low levels of phosphorous, titanium, vanadium and chromium in Siahkooh iron ore compared with level and ratios of these elements in igneous deposits of iron rejects any magmatic origin of this deposit. Ti is an immobile trace element in hydrothermal fluids and can be used as a measure indicator for the amount of clastic materials mixed with deposits (Sugisaki, 1984).

Paragenesis of Mo, Li, Cu, Ba, V, Zn, As, Sb, Pb is one of obvious features of hydrothermal deposits (Monteiro *et al.*, 2008). Distribution pattern of lead, zinc, copper and silver in samples of Siahkooh ore is very similar to hydrothermal iron deposits in the world. Small igneous masses at distances of several hundred meters of iron deposit can be considered as the source of metallic materials, temperature and a part of ore-bearing fluid. Sudden decrease in temperature, PH changes in ore-bearing fluid and probably pressure are the main factors in these metals, deposition (Monteiro *et al.*, 2008).

REFERENCES

Bonatti E, Kramer T and Tydell H (1972). Classification and genesis of submarine iron- manganese deposits. In: *Ferromanganese Deposits on the Ocean Floor: Palisides*, edited by Horn DR, N.Y., *Lamont-Doherty observatory*, *Columbia Uni*. 149-165.

Crerar DA, Namson J, Chyi MS, Williams L and Feigenson MD (1982). Manganiferous cherts of ranciscan Assemblage: I. General geology, ancient and modern analogies, and implication for hydrothermal convection at oceanic spreading centers. *Economic Geology* **77** 519-540.

Goldfarb RJ and Richards JP (No Date). *Economic Geology, 100th Anniversary volume SEG, Denver (page Number?)*

Gholami M and Aftabi A (2010). The geochemical nature of hematite veins of Baghin, Rafsanjan and Kerman. 29th Symposium of Geosciences, *Geological Survey of Iran*, Tehran.

Guilbert JM and Park CF (1997). *The Geology of Ore Deposits* (W. H. Freeman & Co) 984.

Marschik R, Spikings R and Kuscu I (2008). *Geochronology and Stable Isotope Signature of Alteration Related to Hydrothermal Magnetite Ores in Central Anatolia*, Turke, Miner Deposita **43** 111-124.

Monteiro LVS, Xavier RP, Hitzman MW, Juliani C, Filho CRS and Carvalho ER (2008). Mineral chemistry of ore and hydrothermal alteration at the Sossego iron oxide-copper-gold deposit, Carajas Mineral Province, Brazil. *Ore Geology Reviews* **34** 317-336.

Nasr Isfahani AK and Ahmadi M (2005). *Petrography of Igneous Rocks*, Islamic Azad University, (Khorasgan branch publications) Isfahan 262.

Nicholson K (1992). Contrasting mineralogical-geochemical signature of manganese oxide: Guides to metallogenesis. *Economic Geology* **87** 1253-1264.

Robb L (2005). *Introduction to Ore-forming Processes* (Blackwell Publishing) Malden, Maryland.

Roy S (1980). Genesis of sedimentary manganese formations: Processes and products in recent and older geological ages. In: *Geology and Geochemistry of Manganese*, edited by Varentsov IM and Grasselly GY, Akademial Kiado, Budapest **2** 13-44.

Sugisaki R (1984). Relation between chemical composition and sedimentation rate of Pacific ocean-floor sediments deposited since the Middle Cretaceous: Basic evidence for chemical constraints of depositional environments of ancient sediments. *Journal of Geology* **92** 235-259.

Torabian S (2007). Mineralization and genesis of anomaly no. 3 of Gol e gohar iron mine in Sirjan based on distribution of trace elements, MSc thesis, Teacher Training University.

Williams PJ, Barton MD, Johnson DA, Fontbote L, de Haller A, Mark G, Oliver NHS and Marschik R (2005). Iron oxide copper-gold deposits: Geology, space-time distribution and possible modes of origin. In: Hedenquist JW and Thompson JFH